2010

CEST and PARACEST MR Contrast Agents

Ileana Hancu
GE Global Research Center

W. Thomas Dixon
GE Global Research Center

Mark Woods
Portland State University, mark.woods@pdx.edu

Elena Vinogradov
Beth Israel Deaconess Medical Center

A. Dean Sherry
University of Texas at Dallas

See next page for additional authors

Citation Details

Published as: Hancu, I., Dixon, W. T., Woods, M., Vinogradov, E., Sherry, A. D., & Lenkinski, R. E. (2010). CEST and PARACEST MR contrast agents. Acta radiologica (Stockholm, Sweden : 1987), 51(8), 910–923. https://doi.org/10.3109/02841851.2010.502126

Published in final edited form as:

Acta Radiol. 2010 October ; 51(8): 910–923. doi:10.3109/02841851.2010.502126.

CEST and PARACEST MR contrast agents

Ileana Hancu[1], **W. Thomas Dixon**[1], **Mark Woods**[2], **Elena Vinogradov**[3], **A. Dean Sherry**[2,4], and **Robert E. Lenkinski**[3]

[1]GE Global Research Center, Niskayuna, NY

[2]University of Texas at Dallas, Dallas, TX

[3]Beth Israel Deaconess Medical Center, Boston, MA

[4]University of Texas Southwestern Medical Center, Dallas, TX, USA

Abstract

In this review we describe the status of development for a new class of magnetic resonance (MR) contrast agents, based on chemical exchange saturation transfer (CEST). The mathematics and physics relevant to the description of the CEST effect in MR are presented in an appendix published in the online version only. We discuss the issues arising when translating *in vitro* results obtained with CEST agents to using these MR agents in *in vivo* model studies and in humans. Examples are given on how these agents are imaged *in vivo*. We summarize the status of development of these CEST agents, and speculate about the next steps that may be taken towards the demonstration of CEST MR imaging in clinical applications.

Keywords

Model studies; paramagnetic agents; magnetization transfer; target image

Contrast in magnetic resonance (MR) images is largely determined by two factors: the proton density of the tissue under examination, and the relaxation properties of its protons. Conventional contrast agents now widely used in clinical practice work by shortening the longitudinal and/or transverse relaxation times of the protons in their close proximity.

While highly useful for the detection of a number of pathologies, such as cancers (1, 2), multiple sclerosis (3), and cartilage disease (4), these relaxation agents have a number of shortcomings. First, the detection of the agent-induced contrast usually relies on the acquisition of precontrast images to help match and identify the enhanced region (once the agent is injected, its contrast cannot be turned off). As a consequence, unambiguous contrast detection requires relatively large agent doses. Second, although relaxation-based agents responsive to the state of their environment (e.g. pH, temperature, etc.) are being developed (5), the measured effect is a function of both the environment and the agent concentration,

Robert E. Lenkinski, Beth Israel Deaconess Medical Center, 330 Brookline Avenue, Boston, MA 02215, USA (tel. +1 617 667 0274, fax. +1 617 667 7917, rlenkins@bidmc.harvard.edu).

Declaration of interest: The authors report no conflicts of interest. The authors alone are responsible for the content and writing of the paper.

which is usually unknown *in vivo*. This leads to the difficulty of quantification of the environmental parameter of interest. And third, targeted relaxation contrast agents (6) allow the imaging of only one target per MRI exam.

All of these shortcomings can in principle be addressed by a new class of MR contrast agents called chemical exchange saturation transfer (CEST) agents. These new agents introduce image contrast in a fundamentally different way. Their action is not based on proton relaxation; instead, they work by selectively reducing the magnetization of the water signal, with minimal effects on its longitudinal relaxation rate. This is achieved by using molecules that contain exchangeable protons, and a nuclear magnetic resonance (NMR) technique introduced by FORSÉN & HOFFMAN in 1963 (7), called magnetization transfer NMR (MT-NMR).

MT-NMR was revisited by BALABAN et al. in 2000 (8), who named the contrast enhancement procedure chemical exchange saturation transfer (CEST). This name was selected to differentiate the approach from a different kind of MT effect in which radiofrequency (RF) irradiation of the macromolecules transfers magnetization through predominantly cross-relaxation pathways rather than direct chemical exchange (9).

CEST contrast in MR relies on the existence of at least two pools of protons with different NMR chemical shifts (Fig. 1). One pool is made up of the exchangeable protons of the contrast agent which we refer to as “pool A” throughout this review. The second pool is the endogenous bulk water that we refer to as “pool B.” If proton spins in pool A are saturated by a continuous frequency-selective RF saturation pulse, exchange of protons from pool A to pool B during this saturation period decreases the intensity of pool B spins.

For maximum CEST efficiency, the chemical system must be exchanging slowly on the NMR chemical shift time-scale, i.e. $\tau_A \Delta\omega \geqslant 1$ ($\tau_A = 1/k_A$ = lifetime of protons in pool A; $\Delta\omega$, chemical shift difference between the two pools). A good CEST contrast agent must, therefore, possess mobile protons that exchange with water as fast as possible before exchange broadening makes selective RF presaturation ineffective. Larger frequency separations permit shorter proton lifetimes and thus result in larger CEST effects.

There are two main classes of CEST agents: diamagnetic and paramagnetic agents. Although both types of CEST agents rely on exchanging protons, the nature of the exchanging protons is different in the two groups. Diamagnetic agents (DIACEST agents, which can be small or large molecules) typically rely on exchanging protons belonging to −NH and −OH groups whose signals are usually within 5 ppm of the water signal. This relatively small chemical shift difference requires slow exchange rates that, in turn, limit the observed effect per given injected agent dose. Paramagnetic (PARACEST) agents are chelates of paramagnetic (lanthanide) ions that induce much larger shifts in the ligand protons up to a few hundred ppm, depending on the lanthanide structure, thus allowing much shorter proton lifetimes that still obey the slow exchange condition. PARACEST can be single metal-containing chelates, dendrimers, supramolecules, and liposomes, as discussed later.

This review discusses the state of the art of CEST agents. For convenience we have included a description of the mathematics and physics of the CEST effect in the Appendix, available in the online version of this article: http//www.informahealthcare.com/10.3109/02841851.2010.502126.

Development of CEST contrast agents for MRI

The first CEST agents were diamagnetic small molecules (DIACEST) containing exchangeable −NH or −OH protons, reported by WARD et al. in 2000 (8). Since that time there have also been reports of endogenous DIACEST agents. For a typical DIACEST agent, whether endogenous or exogenous, the chemical shift difference ($\Delta\omega$) between the exchangeable −NH or −OH groups and the bulk water is less than 5 ppm, corresponding to ~315 Hz at 1.5 T. Using the slow to intermediate exchange conditions of $\Delta\omega\tau_A \geqslant 1$ as a rough boundary condition for CEST, one would expect CEST to arise only for protons sites with an exchange rate in the order of $\sim 2 \times 10^3\ s^{-1}$ or lower, corresponding to residence lifetimes (τ_A) of ~500μs or longer. This range happens to encompass the exchange lifetimes observed for many types of −NH groups and some −OH groups.

However, the relatively small chemical shift difference of DIACEST agents is their major disadvantage, since the activation of these exchange groups by semi-selective B_1 pulses usually also results in partial saturation of bulk water protons (10). This is most problematic *in vivo* where the bulk water proton signal tends to be rather broad. The control experiment may also partly saturate the agent-bound protons. Typically two irradiations are needed to extract the contrast due to DIACEST agents and calculate the % contrast according to Equation 4 in the Appendix. The Appendix is available in the online version of this article: http://www.informaworld.com/10.3109/02841851.2010.502126.

The small chemical shift of −NH and −OH protons means that the CEST effects of exogenous contrast agents often overlap with strong endogenous MT effects; the separation of the two is needed, hence making the detection of the agent more difficult. On the other hand, DIACEST agents do not require a paramagnetic metal ion to generate the contrast and, therefore, impose no (or reduced) risk of potential toxicity of the contrast agents in the body.

Ideally one would like to increase $\Delta\omega$ as much as possible so that the direct saturation of water does not arise. This can be achieved by using paramagnetic contrast agents (PARACEST agents). The difference between $\Delta\omega$ values of a pair of typical DIACEST and PARACEST agents is illustrated in Fig. 2.

Fig. 2 clearly shows that CEST activation can be performed much more selectively with the PARACEST agent. By expanding the chemical shift difference between the two exchanging pools, more rapidly exchanging systems can be used as CEST agents. For example, if $\Delta\omega$ is increased by a factor of 10 to 50 ppm (equivalent to 3150 Hz at 1.5 T), then the agents with exchange lifetimes as short as ~50 s would also meet the slow to intermediate exchange condition of $\Delta\omega\tau_A \geqslant 1$. Consequently, greater image contrast may be obtained for a given agent dose, assuming sufficient RF saturation is provided. Additionally, the larger distance

of the shifted protons from the bulk water signal means significantly reduced MT effects from tissue (9).

DIACEST contrast agents

Several classes of diamagnetic CEST compounds have been reported to date including both exogenous and endogenous molecules. The exogenous DIACEST agents include small and large synthetic molecules, and reporter genes with DIACEST polymer products, as discussed briefly below. Endogenous DIACEST agents include proteins, glycogen, and glucosaminoglycans. DIACEST agents can be used to image their own presence, the presence of other compounds, or environmental factors such as pH, temperature, transplanted cells, and progenies of transplanted cells.

Small molecule DIACEST contrast agents

In the first report of diamagnetic CEST agents by WARD et al., candidate molecules were chosen based on chemical shift of their exchangeable protons, their rate of chemical exchange, and the need to avoid the rapid exchange limit (8). The 35 compounds chosen in this first report included sugars, amino acids, neucleocides and their bases, and other compounds.

Later, the same group studied a number of pH-responsive CEST agents, including 5,6-dihydrouracil, 5-hydroxytryptophan, and a combination of 5-hydroxytryptophan and 2-imidazolidinethione (Fig. 3). They demonstrated that the CEST agent effect on signal intensity depends not only on the parameter of interest (here pH), but also on the agent concentration, which is always unknown *in vivo* (11). Among these, 5,6-dihydrouracil is a dual CEST agent having two exchangeable protons with exchange rates having different pH dependence. The chemical shift separation of these two exchanging sites is sufficient for selective independent saturation of the two resonances, thus allowing the measurement of two individual CEST effects. Dividing one effect by the other cancels the concentration effect, thus allowing pH determination by calibration.

Macromolecular DIACEST contrast agents

Cationic polymers bind DNA and transport it across cell membranes *in vivo*, and GOFFENEY et al. showed that cationic polyamides (Fig. 4) used as gene transport agents can also serve as CEST agents (12). The large number of amide protons endows these polymers with very high sensitivity. Predictably, agents with slower exchange kinetics (10 s^{-1}) produced weaker CEST effects, and those with more rapid exchange rates (80–140 s^{-1}) had stronger effects. Polymers that exchanged too rapidly to produce a separate observable resonance for pool A failed to produce any observable CEST effect.

The benefit of signal amplification by polymeric species also applies to PARACEST agents, as mentioned later for Yb^{3+}-DOTAM (13).

Reporter gene DIACEST contrast agents

Labeling cells for imaging their location, migration pattern, and viability represents an active area of MRI research. Most relaxation and CEST contrast agents produce a finite effect that undergoes dilution following the division of the labeled cells. This is not necessarily the case for genes encoding for CEST agents. For instance, Rat 9L-glioma cells labeled with the gene encoding for green fluorescent protein and for a lysine-rich protein (LRP), were transplanted into a mouse brain and allowed to grow into a tumor (14). CEST images showed this tumor but not similar tumors grown from control cells. The high sensitivity of the LRP reporter gene relative to other cell proteins is explained as follows: LRP has many amide protons, all resonating within a small spectral range of about 3.76 ppm from water, as compared with the broader spectral range of naturally occurring amides. Moreover, the genetically engineered gene reporter has faster exchange kinetics than the average amide proton, thus resulting in a stronger CEST effect than that of native proteins.

This approach of modifying genes to encode for CEST agents has the added potential of imaging cell viability. As healthy cells divide, more LRP is produced, leading to correspondingly larger observed CEST effect. Moreover, at physiological pH the amide proton exchange is base catalyzed; if the labeled cells migrate to a low pH ischemic environment, their detectability by CEST imaging is reduced up to 10-fold for a 1 pH unit. Similar effects have also been demonstrated with genes encoding for optical markers; however, these markers can only be detected at shallow depths, even with near infrared light. Genes encoding for CEST-active proteins are potentially useful for noninvasive whole-body imaging.

Paramagnetic lanthanide complexes as PARACEST agents

Paramagnetic lanthanide ions first made an impact in NMR during the early 1970s, with the discovery of lanthanide shift reagents (SRs) (15). The first SRs were organic soluble Lewis acid-type complexes that spread the proton resonances of organic molecules, essentially turning low field nonfirst order NMR spectra into the equivalent of high field first order spectra (15, 16). Later it was found that the hyperfine shifts induced by the lanthanide aqua ions were also useful in resolving the structures of molecules, such as nucleic acids, peptides, proteins, and other biological molecules (17). The hyperfine shifts induced by lanthanide ions in proton resonances of a molecule can be quite large, up to several hundred ppm, especially for protons that are part of the lanthanide complex itself or when the lanthanide is tightly bound at a specific protein binding site.

The next important milestone in NMR application of lanthanides was the introduction of Gd^{3+} complexes as contrast agents for MRI in the early 1980s (18). Gd^{3+} has seven unpaired electrons equally distributed in its 7f orbitals (isotropic), and hence cannot induce hyperfine shifts like other lanthanides. Gd^{3+} does, however, have a profound effect on the relaxation rates of nearby nuclei in a complex or any molecule that binds to it or diffuses near the Gd^{3+} complex. This is the foundation for use of Gd^{3+} as T_1 contrast agents for medical MRI (19, 20).

Other paramagnetic lanthanides had enjoyed far fewer applications in imaging until the discovery of PARACEST (21). As illustrated above, Δω is an important parameter in CEST applications, so the same hyperfine shifting characteristics of lanthanide ions have once again become the focus of attention. The CJ constants (Table 1) derived by BLEANEY et al. (22, 23) provide a useful reference for predicting the relative hyperfine shifting ability of various lanthanide cations.

Modulation of water exchange rates in lanthanide complexes

An important physical characteristic of lanthanides as PARACEST contrast agents is the rate of water exchange in their complex. Interestingly, however, fast water exchange that is desirable to increase the relaxivity of Gd^{3+}-based T1 agents is detrimental in PARACEST-based systems. In fact water exchange in lanthanide complexes was considered much too fast for CEST imaging until the discovery that the exchange rate in Gd^{3+} complexes of bis-amide derivatives of diethylenetriamine pentaacetate (DTPA), such as gadolinium(III) diethylenetriamine pentaacetate-bismethyl amide (GdDTPA-BMA) is unexpectedly slow, with τ_A values in the range of 1–3μs (24). This realization opened the door to comprehensive studies of water exchange rates in lanthanide complexes. For instance, Eu^{3+} complexes of DOTA-tetraamide derivatives, a representative structure of which is shown in Fig. 2, have been reported with bound water lifetimes as slow as 200–300μs; clearly, such slow water exchange makes these complexes suitable for PARACEST imaging applications (21).

Lanthanide complexes that are stable enough for *in vivo* applications have one water molecule coordinated directly to the metal ion (20), which exchanges with the bulk water molecules. The rate of water exchange is in direct relationship to the metal ion's requirement for electron density from the water molecule. Thus, the extent to which other ligands provide electron density to the metal ion influences the water exchange rate and the CEST effect.

For instance, consider the ligand series shown in Fig. 5, which contains a carboxylate, amide or keto group. The carboxylate group, as in DTPA or DOTA ligands, contributes the most electron density to the lanthanide ion, which results in complexes that exhibit the fastest water exchange in this series. The ligand containing the amide group has a somewhat slower water exchange because amide oxygens are much weaker electron donors than carboxylates. This increases the demand for electrons from the water molecule on the lanthanide ion. Thus, ligands with ligating amide group, as in diethylenetriamine pentaacetate-bismethyl amide (DTPA-BMA) or DOTA-tetraamides, have much slower water exchange (24, 25). Although water-soluble ketone-type systems have not, to our knowledge, been reported, one would predict that such ligands would display the slowest water exchange of the series due to their very poor electron donor character.

Design and development of responsive PARACEST agents

If the water exchange rate (k_A) or the chemical shift difference (Δω) of a CEST agent can be induced to change in response to a change in a biologically important variable, then it should be possible to design biologically responsive CEST agents. There are a number of

approaches to altering water molecule or proton exchange in PARACEST agents, among which three examples (26–29) are illustrated in Fig. 6.

As mentioned above, the strength of the lanthanide–water interaction affects the rate of water exchange in Eu-DOTA-tetraamide complexes that undergo dissociative exchange. The strength of interaction in these complexes can be modulated by altering the electronic effects of an aromatic amide substituent (26). As shown in Fig. 6a, a p-NO_2-phenyl (electron-withdrawing) amide substituent yields a PARACEST agent with slower water exchange compared with an agent containing a p-NH_2-phenyl (electron-donating) substituent, and this difference is easily detected by CEST imaging. This observation suggests that properly designed responsive agents may enable detection and measurement of tissue characteristics, such as redox potential, O_2, or other biological indexes of interest.

A second example of a responsive PARACEST agent iseuropium(III)1,4,7,10-tetraazacyclocodecane-1,7-di-N-butylacetamide-4,10-di-N-[ethyl(dimethylpyridine) amino]acetamide (Eu-D2BAM-2BiPyAM) designed to sense Zn^{2+} ions. Here the four pyridyl groups positioned above the water coordination site of Eu bind a Zn^{2+} ion (28). This arrangement places a zinc-coordinated −OH group just above the Eu^{3+}-bound water molecule, which appears to catalyze the exchange of protons between the Eu^{3+}-bound water molecule and bulk water (Fig. 6b). In this complex the CEST is “on” in the absence of Zn^{2+}, but it is turned “off “ when the catalytic −OH group is introduced by Zn^{2+}.

In a similar way, a suitable compound can be arranged above the Eu^{3+}-bound water molecule to slow down the water exchange and turn on the CEST effect. One example of such a system is given by the glucose-responsive PARACEST agent europium(III) 1,4,7,10-tetraazacyclododecane-1,7-di-*N*-methylacetamide-4, 10-di-*N*-(*m*-phenylboronate)acetamide (Eu-D2MA-2PB) (21, 29), in which a single glucose molecule is bound by two phenylboronate groups above the Eu^{3+}- water binding site. Phenylboronate groups form strong complexes with cis-dihydroxy compounds, such as sugars. These examples indicate that chemical exchange is relatively easy to modify in these complexes and that a variety of responsive agents can be envisioned for sensing various biological indexes of importance.

Many organic-based bis-phenylboronate structures display high affinity for binding fructose, but europium(III) 1,4,7,10-tetraazacyclododecane-1,7-di-*N*-methylacetamide-4,10-di-*N*-(m-phenylboronate) acetamide (Eu-D2MA-2PB, Fig. 7) has a preference for binding glucose over fructose (29). This surprising result indicates that phenylboronate rings of Eu-D2MA-2PB are oriented in such a way that their condensation with the cis-hydroxy groups of glucose is more favorable than with the cis-hydroxy groups of fructose.

Examination by ultraviolet absorption and circular dichroism spectroscopy confirmed that a 1/1 Eu-D2MA-2PB–glucose adduct is the predominant structure in solution, with the glucose most likely bound via its 1,2-cis-hydroxy groups to one phenylboronate and via the 4,6-cis-hydroxy groups to another phenylboronate. The steric encumbrance that arises from the position of the glucose molecule hinders the dissociation of the bound water molecule, thus slowing down water exchange. In this example, water exchange rate is reduced by a factor of about 2 when glucose is bound, and this is sufficient to “turn on” CEST function in

the complex. This agent has been used to monitor the distribution of tissue glucose in isolated perfused mouse livers, as illustrated in Fig. 7 (27).

PARACEST agents with nonwater exchange sites

PARACEST agents may contain secondary exchanging sites in addition to that of their water exchange site. One such example is the Yb-DOTA-tetraamide complex, discussed above, in which the amide protons of the pendant arms not only exchange with the bulk water but also experience a significant hyperfine shift from the lanthanide ion. Although the magnitude of the hyperfine shift is smaller than that of the bound water molecule, these protons are still useful for CEST activation. First, there are four or more amide protons compared with two in bound water protons. Second, unlike CEST from bound water, CEST arising from the amide protons have a marked pH dependence, just as in simple DIACEST systems (11, 30, 31).

Thus, there is now considerable interest in amide protons of DOTA-tetraamide complexes for developing methods to image tissue pH *in vivo* (30). An interesting example of such a pH-responsive PARACEST agent is provided by a series of dendrimers bearing Yb-DOTAM complexes, as depicted in Fig. 8 (13). Here the pH sensitivity depends on the generation of the dendrimer, which may allow some structure tuning for optimum effect.

The amide protons of the Yb-DOTA-tetraamide complex are highly shifted (~ –20 ppm), and by attaching a large number of complexes on the surface of a dendrimer, a considerable enhancement in sensitivity can be achieved, depending on the size of the dendrimer.

Supramolecular and liposome-based CEST agents

Highly sensitive CEST agents were recently developed by moving beyond the simple complex towards supramolecular structures. Initially Aime and co-workers proposed ion-paired assemblies of poly-L-arginine and Tm^{3+}-DOTP (32) as CEST agents. A different supramolecular approach, dubbed LIPOCEST, was reported 2 years later and involves the incorporation of a shift reagent, such as Tm^{3+}-DOTMA, inside a liposome (33). Liposomes are vesicular structures in the size range of about 50–300 nm (Fig. 9) comprising one or more phospholipid bilayers. The bilayer(s) enclose an inner aqueous pool that can be loaded with various water-soluble compounds. The liposomal wall is permeable to water, allowing water molecules of the inner aqueous environment of the liposomes to exchange with bulk water. A water-soluble paramagnetic shift reagent then shifts the resonance frequency of the encapsulated water away from the resonance frequency of bulk water, allowing selective saturation and LIPOCEST to be generated.

However, due to osmotic pressure limitations on agent concentration inside the liposomes, a strongly shifting lanthanide is needed to shift the Larmor frequency sufficiently, so that the RF pulse can saturate the liposome contents without saturating the bulk tissue water. Efficient PARACEST agents require lanthanides, such as Eu^{3+}, with long water-binding lifetimes to allow the selective saturation of the bound proton pool. LIPOCEST agents have a similar requirement, as the water inside the liposomes behaves as a single pool shifted by the paramagnetic agent. The exchange time between intra-liposomal water and bulk tissue

water should be rapid but at the same time slow enough for selective saturation by an RF pulse. This is similar to the PARACEST case where the exchange rate must allow selective saturation.

In DIACEST and PARACEST the exchange time is controlled by the chemical properties of the agent. In LIPOCEST the exchange time is mainly determined by the chemical structure and architecture of the phospholipid bilayer of the liposome and by their surface-to-volume ratio. In the first LIPOCEST experiment, Tm-DOTMA at a concentration of 0.1 M was used as a shift reagent within the liposomes (mean diameter of 270 nm), resulting in the liposomal water resonating 3.1 ppm downfield from the bulk water outside the liposomes (33). Although the exchange rate was not reported, the Z spectrum of the aqueous dispersion of the liposomes containing the Tm complex recorded at 600 MHz shows a clear separation between the peaks of the free bulk water and the water within the liposome, as shown in Fig. 9.

The sensitivity of this type of agent can be improved by increasing the average chemical shift of water within the liposomes that is proportional to Ln^{3+} concentration. Since this concentration is limited by osmosis, neutral shift reagents that do not require counter ions are preferable. Dimeric and trimeric shift reagents allow higher intra-liposomal lanthanide concentrations without the concomitant increase in osmolality. TERRENO et al. examined the effect of a dimeric shift reagent that was able to provide approximately twice the shift of a monomeric reference compound (34). However, a trimeric shift reagent was found to be only slightly more effective than the dimer, a result of the ligand structure chosen for the central lanthanide ion. The structure of the liposome bilayer can also influence the CEST effect. Amphiphilic shift reagents, for instance, can associate with the phospholipid wall, with the hydrophobic tail buried within the phospholipid wall, and the more polar shift reagent segment pointing out into the aqueous environment. This increases the total lanthanide concentration within the liposomes; the agent concentration per unit wall area is not limited by osmosis.

A further consideration in LIPOCEST is the size and shape of the liposomes. Provided that an adequate chemical shift is generated, smaller liposomes have the additional advantage of higher surface-to-volume ratio, and hence, faster exchange and a stronger CEST effect (35). Non-spherical liposomes can be used to induce larger chemical shifts by taking advantage of bulk magnetic susceptibility effects. Incorporating gadolinium 1,4,7,10-tetraazacyclododecane-1-hydropropyl-4,7,10-triacetate (Gd-HP-DO3A) at 0.1 Osmol into a spherical liposome does not give rise to a shift in the intraliposomal water signal. However, incubation of the liposomes in an isotonic solution (0.28 Osmol) causes intraliposomal water to be expelled until the liposome interior is also 0.28 Osmol. This osmotic stress produces nonspherical liposomes and induces susceptibility effects that shift the resonance frequency of the intraliposomal water about 8 ppm downfield – double the shift achieved by the first experiment (36).

The shifts that can be generated by osmotically deforming the liposomes can be increased still further by using wall-bound amphiphilic shift reagents (37). This approach also permits control of the direction of the induced chemical shift, allowing the simultaneous detection of

two different agents in the same environment, which is an important CEST imaging capability (38). Liposomes were prepared incorporating either the thulium(III) or dysprosium(III) complexes of 1,4,7,10-tetraazacyclododecane-1-dihexadecylacetamide-4,7,10-triacetate into the liposome wall and entrapping an aqueous solution of HP-DO3A complex of the same Ln^{3+} ion. After osmotic stress, the chemical shift of water within the nonspherical liposomes is shifted upfield in those liposomes containing Dy^{3+} but downfield in those containing Tm^{3+}. Shifts as large as 45 ppm could be achieved by this method (37). Preparations of these nonspherical liposomes, one containing Dy^{3+} and the other Tm^{3+}, were co-injected into a sample of beef and followed by CEST imaging, which showed the location of the injection. The Z spectrum of the site showed resolved peaks at 3 and 18 ppm.

In vivo applications of CEST imaging

In vivo imaging of endogenous CEST molecules, including imaging of pathological conditions in humans, is far more advanced than imaging of exogenous CEST agents. Although the focus of this review is exogenous CEST agents, an overview of animal and human experiments based on endogenous CEST molecules is also presented here. However, given the relatively early stage in the development of exogenous CEST agents, the majority of imaging experiments involving exogenous CEST agents is done in phantoms and perfused tissues. A few examples of *in vivo* images acquired in animal models are also presented, but as yet there is no reported imaging of exogenous CEST agents in humans.

In vivo imaging of endogenous biomolecules

Living organisms contain many proteins whose amide −NH protons exchange with water at rates suitable for CEST imaging. RF saturation of these endogenous resonances can provide useful information, even when the particular amide containing molecules is unknown. For instance, ZHOU et al. have reported that amide proton transfer (APT) in rat brain changes with pH during ischemia (39). JONES et al. also used this method to examine the difference between protein contents of brain tumor and its surroundings in patients at 3T (40).

Glycogen (a branched polymer of glucose), with its many −OH groups, is also an interesting endogenous CEST agent. Glycogen stores glucose in the liver, skeletal muscle, heart, and brain; its concentration is affected by diabetes, an all too common condition, and by several rare diseases. VAN ZIJL et al. have reported that CEST (glycoCEST) can be observed from the exchangeable –OH groups of glycogen in perfused mouse liver and that the glycogen content decreases when the liver is perfused with a glucose-free medium (41). ^{13}C spectroscopy can also be used to assess *in vivo* glycogen noninvasively, but few clinical scanners have the necessary hardware for such investigations.

Glucosaminoglycans (GAGs) are another class of endogenous CEST molecules that are abundant and important to the function of several tissues, including cartilage. Each repeating unit of GAGs contains one –NH and three potentially CEST active –OH protons. The –NH proton is shifted 3.2 ppm relative to bulk water signal, and the –OH proton 0.9–1.9 ppm. LING et al. were able to observe “gagCEST” effects from –OH protons of GAG in the cartilage of both bovine specimens and in the knee of a human volunteer following

irradiation at 1 ppm away from the water resonance (42). This gagCEST effect could be observed in cartilage at 500 and 200, and even at 127 MHz (at 3 T) at which field the water and –OH resonances were only 64 Hz apart.

Conventional wisdom suggests that, in order for the CEST effect to be observable, chemical exchange should be slow, resulting in narrow resonances well separated from that of water. Typically –OH proton exchange rates are ~1000/s; thus, for both gag- and glycoCEST, the slow exchange condition has been breached. The glycoCEST paper (41) confirms that the –OH line is not seen at all in a standard 1H NMR spectrum, confirming the violation of the slow exchange condition. This fact complicates quantification (not attempted in either of the above-mentioned experiments) but clearly does not abolish the CEST effect.

In vivo imaging of reporter genes

As described earlier, cells can be genetically modified to express proteins that can be imaged by CEST. The LRP reporter was the first to be imaged in 2007 by using APT for labeling of the amide protons of this reporter (14). Both the cells expressing LRP and control xenografts were inoculated in opposite sides of a mouse brain, followed by CEST signal intensity-difference mapping, as shown in Fig. 10. This is the first example of a reporter gene targeted specifically for MRI-related investigation. It is a prototype CEST imaging of reporter genes that may have application in cell tracking and monitoring of gene expression and delivery.

In vivo imaging of PARACEST agents

In vivo retention and accumulation of PARACEST agents

The use of PARACEST agents in imaging generally suffers from low sensitivity and temporal resolution. Sensitivity can be improved by the use of agents that accumulate in the diseased tissue at higher concentrations, and agents with long *in vivo* retention times may be used to compensate for poor temporal resolution. One PARACEST agent reported by ALI & PAGEL to have both of these properties is europium(III) 1,7-bis[2-(methylene benzyloxy ether)-acetic acid] acetamide-4,10 bis(acetamidoacetic acid)-1,4,7,10-tetraazacyclododecane (Eu-DOTAM-OBnS_2-Gly_2-COOH) (43). The dynamic pharmacokinetics of the agent was successfully monitored in the vena cava, liver, and kidneys of mice by MRI. PARACEST effect was observed in the kidney cortex within 40 s post-injection, reaching maximum at 4.6 min, and disappearing by 8.6 min. A 6–8% PARACEST effect in the liver could still be observed 30 min post-injection.

On-resonance paramagnetic chemical exchange effect

Achieving an observable PARACEST effect for fast exchanging complexes of Tm and Dy may require the application of RF saturation pulses that exceed the specific absorption rate (SAR) imposed limit, thus precluding their use in humans. However, an alternative methodology that would allow detection of these agents *in vivo* has recently been introduced; the method is termed “on-resonance paramagnetic chemical exchange effect”, hence, the acronym OPARACHEE (44). As the name implies, the method involves an “RF irradiation train” on free water resonance.

Two of the main features of this new method are (i) much lower RF power deposition, and (ii) elimination of the need for a priori knowledge of the exact frequency of the lanthanide-bound proton resonances. A broadband composite pulse decoupling scheme (WALTZ-16* pulse-train), is employed in this method, as the composite pulse train compensates for both B_1 and B_0 inhomogeneities (45, 46).

In vitro studies with thulium(III) [1,4,7,10-tetraazacyclododecane-1,4,7,10-tetraacetamide] (Tm-DOTAM) and Dy-DOTAM show that OPARACHEE can detect agent concentrations of about 12 μM (44). The sequence was tested *in vivo* with a Tm-DOTAM-Gly compound, and the clearance of the agent through the mouse kidney was monitored (Fig. 11). Tm-DOT-AM-Gly compound is sometimes referred to as Tm-DOTA-4AmC.

The lowest detectable dosage was a 2 mM bolus (~0.018 mmole/kg), producing an average maximum signal reduction of ~45% in the papilla of the kidney (47). This is a significant image contrast, so one would reasonably expect that lower doses would still be detectable. However, the application of WALTZ-16* train on free water leads to significant signal reduction due to direct saturation effects. At present, the sequence sensitivity of OPARACHEE is limited by the low SNR, rather than by the size of signal modulation (as opposed to standard PARACEST method).

Concluding remarks

Since the introduction of CEST in 2000, a variety of both diamagnetic (DIACEST) and paramagnetic (PARACEST) agents have been developed, as discussed in this review. The fundamental features that distinguish CEST contrast agents from relaxation contrast agents include the following.

1. Contrast can be turned on and off, thus allowing the acquisition of unenhanced images at the same time – just before or just after the acquisition of enhanced images. These conditions enable digital image subtraction, potentially allowing for smaller enhancement effects to be measurable than is possible with relaxation agents.
2. Methods for development of CEST agents sensitive to environmental parameters, such as pH, temperature, or metabolite concentration, are more versatile than those of responsive relaxation agents. With CEST proton exchange lifetimes can be measured quantitatively, hence giving the possibility of obtaining quantitative maps of the environmental parameter of interest.
3. CEST agents are more versatile for development of multiplex imaging (i.e. imaging multiple targets or process simultaneously) than are relaxation contrast agents, as CEST agents can be designed with differentially resonating exchanging sites, each of which can be targeted to a different site. A cocktail of such agents can then be administered at the same time to a patient for probing different targets, thus slashing the one target per exam limit of relaxation-based agents.

CEST agents present some challenges in terms of application to human studies. Although their theoretical detection limit may be lower than that of relaxation-based agents, their experimental detection limit remains higher, due to practical limitations. While detection of μM concentrations of CEST agents has been reported, experiments have not necessarily been performed within the FDA guidelines for SAR deposition. Consequently, the range of concentrations of CEST agents that can be used safely in humans remains to be established.

In spite of the technical and practical challenges present in translating CEST imaging to human studies there is some evidence to suggest that at least for DIACEST agents this translation is readily achievable. JONES et al. (40) have shown that CEST can be applied to imaging human brain tumors using the CEST effect present from the amide protons of protein rich tumors. We suggest that it is only a matter of time until human “gagCEST” and “glycoCEST” studies appear in the literature. The advent of 7 T whole-body scanners increases the likelihood of the implementation of human CEST studies using endogenous agents.

The application of endogenous PARACEST agents to human studies may require longer stages of development. Both the technical challenges associated with the MR acquisitions of these agents as well as concerns related to the toxicity of these endogenous agents present larger barriers to adoption. However, the promise of responsive agents, together with the theoretical ability to monitor several targets or processes simultaneously, provide a strong motivation for addressing these challenges.

Acknowledgements

This work was supported in part by the National Institutes of Health (NIH) grant no. EB004582. We would like to thank Dr A.K. Grant for the useful discussions on parallel imaging. Contract/grant sponsor: NIH, grant no. 5R01EB004582–03.

References

1. DeMartini W, Lehman C, Partridge S. Breast MRI for cancer detection and characterization: a review of evidence-based clinical applications. Acad Radiol 2008;15:408–16. [PubMed: 18342764]
2. Smirniotopoulos JG, Murphy FM, Rushing EJ, Rees JH, Schroeder JW. Patterns of contrast enhancement in the brain and meninges. Radiographics 2007;27:525–51. [PubMed: 17374867]
3. Bakshi R Magnetic resonance imaging advances in multiple sclerosis. J Neuroimaging 2005;15(4 Suppl):5S–9S. [PubMed: 16385014]
4. Blumenkrantz G, Majumdar S. Quantitative magnetic resonance imaging of articular cartilage in osteoarthritis. Eur Cell Mater 2007;13:76–86. [PubMed: 17506024]
5. Hartman KB, Laus S, Bolskar RD, Muthupillai R, Helm L, Toth E, et al. Gadonanotubes as ultrasensitive pH-smart probes for magnetic resonance imaging. Nano Lett 2008;8:415–19. [PubMed: 18215084]
6. Huinink HP, Sanders HM, Erich SJ, Nicolay K, Strijkers GJ, Merkx M, et al. High-resolution NMR imaging of paramagnetic liposomes targeted to a functionalized surface. Magn Reson Med 2008;59:1282–6. [PubMed: 18421697]
7. Forsen S, Hoffman RA. Study of moderately rapid chemical exchange reactions by means of nuclear magnetic double resonance. J Chem Phys 1963;39:2892–901.
8. Ward KM, Aletras AH, Balaban RS. A new class of contrast agents for MRI based on proton chemical exchange dependent saturation transfer (CEST). J Magn Reson 2000;143:79–87. [PubMed: 10698648]

9. Henkelman RM, Stanisz GJ, Graham SJ. Magnetization transfer in MRI: a review. NMR Biomed 2001;14:57–64. [PubMed: 11320533]
10. Zhang S, Winter P, Wu K, Sherry AD. A novel Europium(III)-based MRI contrast agent. J Am Chem Soc 2001;123: 1517–18. [PubMed: 11456734]
11. Ward KM, Balaban RS. Determination of pH using water protons and chemical exchange dependent saturation transfer (CEST). Magn Reson Med 2000;44:799–802. [PubMed: 11064415]
12. Goffeney N, Bulte JW, Duyn J, Bryant LH Jr, van Zijl PC. Sensitive NMR detection of cationic-polymer-based gene delivery systems using saturation transfer via proton exchange. J Am Chem Soc 2001;123:8628–9. [PubMed: 11525684]
13. Pikkemaat JA, Wegh RT, Lamerichs R, van de Molengraaf RA, Langereis S, Burdinski D, et al. Dendritic PARACEST contrast agents for magnetic resonance imaging. Contrast Media Mol Imaging 2007;2:229–39. [PubMed: 17937448]
14. Gilad AA, McMahon MT, Walczak P, Winnard PT Jr, Raman V, van Laarhoven HW, et al. Artificial reporter gene providing MRI contrast based on proton exchange. Nat Biotechnol 2007;25:217–19. [PubMed: 17259977]
15. Hinckley CC. Lanthanide shift reagents. Proc Rare Earth Res Conf, 10th 1973;1(CONF-730402-P1):362–71.
16. Hinckley CC. Applications of lanthanide shift reagents. Mod Methods Steroid Anal 1973:265–79.
17. Peters JA, Huskens J, Raber DJ. Lanthanide induced shifts and relaxation rate enhancements. Progress in Nuclear Magnetic Resonance Spectroscopy 1996;28:283–350.
18. Lauffer RB. Paramagnetic metal complexes as water proton relaxation agents for NMR imaging: theory and design. Chem Rev 1987;87:901–27.
19. Caravan P, Ellison JJ, McMurry TJ, Lauffer RB. Gadolinium(III) chelates as MRI contrast agents: structure, dynamics, and applications. Chem Rev 1999;99:2293–352. [PubMed: 11749483]
20. Merbach AE, Toth E, editors. The chemistry of contrast agents in medical magnetic resonance imaging New York: Wiley; 2001.
21. Zhang S, Merrit M, Woessner DE, Lenkinski RE, Sherry AD. PARACEST agents: modulating MRI contrast via water proton exchange. Acc Chem Res 2003;36:783–90. [PubMed: 14567712]
22. Bleaney B Nuclear magnetic resonance shifts in solution due to lanthanide ions. J Magn Reson 1972;8:91–100.
23. Bleaney B, Dobson CM, Levine BA, Martin RB, Williams RJP, Xavier AV. Origin of lanthanide nuclear magnetic resonance shifts and their uses. J Chem Soc Chem Commun 1972:791–3.
24. Powell DH, Ni Dhubhghaill OM, Pubanz D, Helm L, Lebedev YS, Schlaepfer W, et al. High-pressure NMR kinetics. Part 74. Structural and dynamic parameters obtained from 17O NMR, EPR, and NMRD studies of monomeric and dimeric Gd3+ complexes of interest in magnetic resonance imaging: an integrated and theoretically self-consistent approach. J Am Chem Soc 1996;118:9333–46.
25. Aime S, Barge A, Bruce JI, Botta M, Howard JAK, Moloney JM, et al. NMR, relaxometric, and structural studies of the hydration and exchange dynamics of cationic lanthanide complexes of macrocyclic tetraamide ligands. J Am Chem Soc 1999;121:5762–71.
26. Ratnakar SJ, Woods M, Kovacs Z, Sherry AD. Modulation of water exchange in Europium(III) DOTA-tetraamide complexes via electronic substituent effects. J Am Chem Soc 2007;130:6–7. [PubMed: 18067296]
27. Ren J, Trokowski R, Zhang S, Malloy CR, Sherry AD. Imaging the tissue distribution of glucose in livers using A PARACEST sensor. Magn Reson Med 2008;60:1047–55. [PubMed: 18958853]
28. Trokowski R, Ren JM, Kalman FK, Sherry AD. Selective sensing of zinc ions with a PARACEST contrast agent. Angew Chem Int Ed Engl 2005;44:6920–3. [PubMed: 16206314]
29. Trokowski R, Zhang S, Sherry AD. Cyclen-based ph0065nylboronate ligands and their Eu3+ complexes for sensing glucose by MRI. Bioconjug Chem 2004;15:1431–40. [PubMed: 15546212]
30. Terreno E, Castelli DD, Cravotto G, Milone L, Aime S. Ln(III)-DOTAMGly complexes: a versatile series to assess the determinants of the efficacy of paramagnetic chemical exchange saturation transfer agents for magnetic resonance imaging applications. Invest Radiol 2004;39:235–43. [PubMed: 15021328]

31. Zhou J, Lal B, Wilson DA, Laterra J, van Zijl PCM. Amide proton transfer (APT) contrast for imaging of brain tumors. Magn Reson Med 2003;50:1120–6. [PubMed: 14648559]
32. Aime S, Delli Castelli D, Terreno E. Supramolecular adducts between poly-L-arginine and [TmIIIdotp]: a route to sensitivity-enhanced magnetic resonance imaging-chemical exchange saturation transfer agents. Angew Chem Int Ed Engl 2003;42:4527–9. [PubMed: 14520757]
33. Aime S, Delli Castelli D, Terreno E. Highly sensitive MRI chemical exchange saturation transfer agents using liposomes. Angew Chem Int Ed Engl 2005;44:5513–15. [PubMed: 16052647]
34. Terreno E, Barge A, Beltrami L, Cravotto G, Castelli DD, Fedeli F, et al. Highly shifted LIPOCEST agents based on the encapsulation of neutral polynuclear paramagnetic shift reagents. Chem Commun (Camb) 2008;7:600–2.
35. Zhao JM, Har-el YE, McMahon MT, Zhou J, Sherry AD, Sgouros G, et al. Size-induced enhancement of chemical exchange saturation transfer (CEST) contrast in liposomes. J Am Chem Soc 2008;130:5178–84. [PubMed: 18361490]
36. Aime S, Delli Castelli D, Lawson D, Terreno E. Gd-loaded liposomes as T1, susceptibility, and CEST agents, all in one. J Am Chem Soc 2007;129:2430–1. [PubMed: 17288421]
37. Terreno E, Cabella C, Carrera C, Delli Castelli D, Mazzon R, Rollet C, et al. From spherical to osmotically shrunken paramagnetic liposomes: an improved generation of LIPOCEST MRI agents with highly shifted water protons. Angew Chem Int Ed Engl 2007;46:966–8. [PubMed: 17167807]
38. Terreno E, Castelli DD, Milone L, Rollet S, Stancanello J, Violante E, et al. First ex-vivo MRI co-localization of two LIPOCEST agents. Contrast Media Mol Imaging 2008;3:38–43. [PubMed: 18335476]
39. Zhou J, Payen JF, Wilson DA, Traystman RJ, van Zijl PC. Using the amide proton signals of intracellular proteins and peptides to detect pH effects in MRI. Nat Med 2003;9:1085–90. [PubMed: 12872167]
40. Jones CK, Schlosser MJ, van Zijl PC, Pomper MG, Golay X, Zhou J. Amide proton transfer imaging of human brain tumors at 3T. Magn Reson Med 2006;56:585–92. [PubMed: 16892186]
41. van Zijl PC, Jones CK, Ren J, Malloy CR, Sherry AD. MRI detection of glycogen in vivo by using chemical exchange saturation transfer imaging (glycoCEST). Proc Natl Acad Sci U S A 2007;104:4359–64. [PubMed: 17360529]
42. Ling W, Regatte RR, Navon G, Jerschow A. Assessment of glycosaminoglycan concentration in vivo by chemical exchange-dependent saturation transfer (gagCEST). Proc Natl Acad Sci U S A 2008;105:2266–70. [PubMed: 18268341]
43. Ali MM, Pagel MD. Longer in vivo retention and accumulation improves detection of PARACEST MRI contrast agents. Proceedings of the International Society for Magnetic Resonance in Medicine, Toronto, 2008.
44. Vinogradov E, Zhang S, Lubag A, Balschi JA, Sherry AD, Lenkinski RE. On-resonance low B1 pulses for imaging of the effects of PARACEST agents. J Magn Reson 2005;176:54–63. [PubMed: 15979362]
45. Shaka AJ, Keeler J, Freeman R. Evaluation of a new broadband decoupling sequence: WALTZ-16. J Magn Reson 1983;53:313–40.
46. Shaka AJ, Keeler J, Frenkiel T, Freeman R. An improved sequence for broadband decoupling: WALTZ-16. J Magn Reson 1983;52:335–8.
47. Vinogradov E, He H, Lubag A, Balschi JA, Sherry AD, Lenkinski RE. MRI detection of paramagnetic chemical exchange effects in mice kidneys in vivo. Magn Reson Med 2007;58:650–5. [PubMed: 17899603]

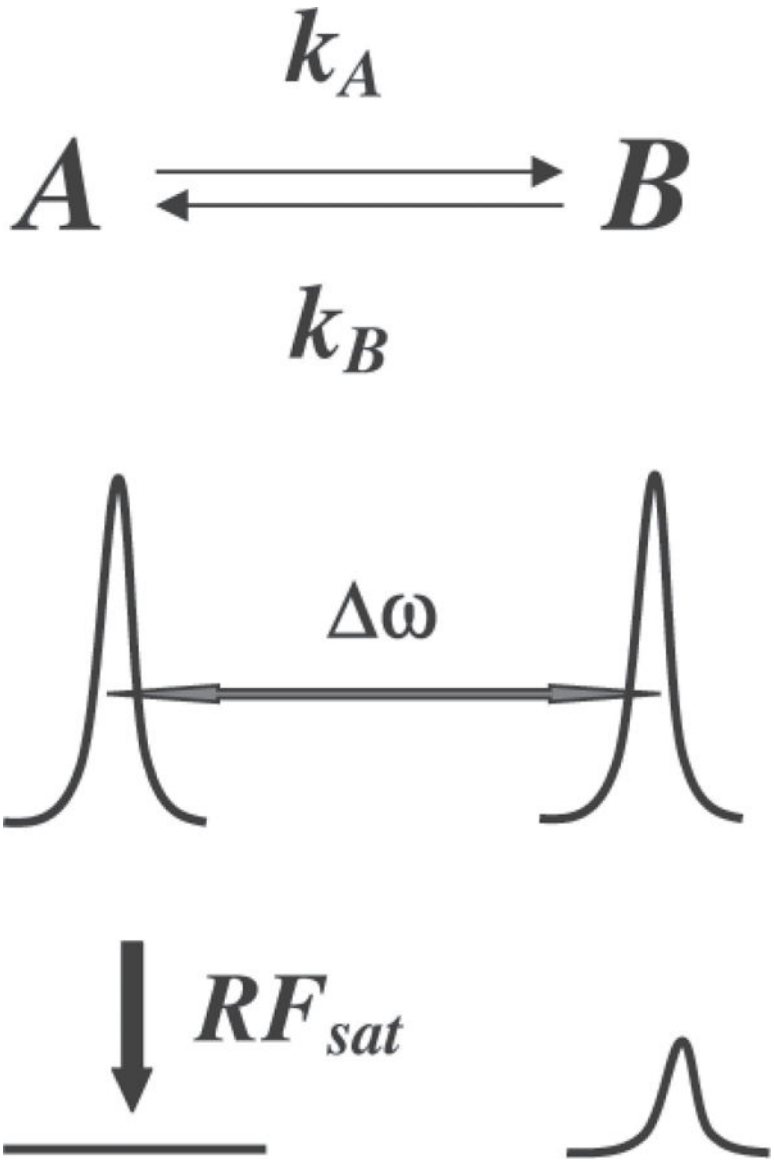

Fig. 1.

Schematic depicting chemical exchange between two pools of spins, separated by Δω (A = exchangeable protons on the agent and B = bulk water). The lower part of the graph depicts a decrease in the pool B signal following selective RF saturation of pool A.

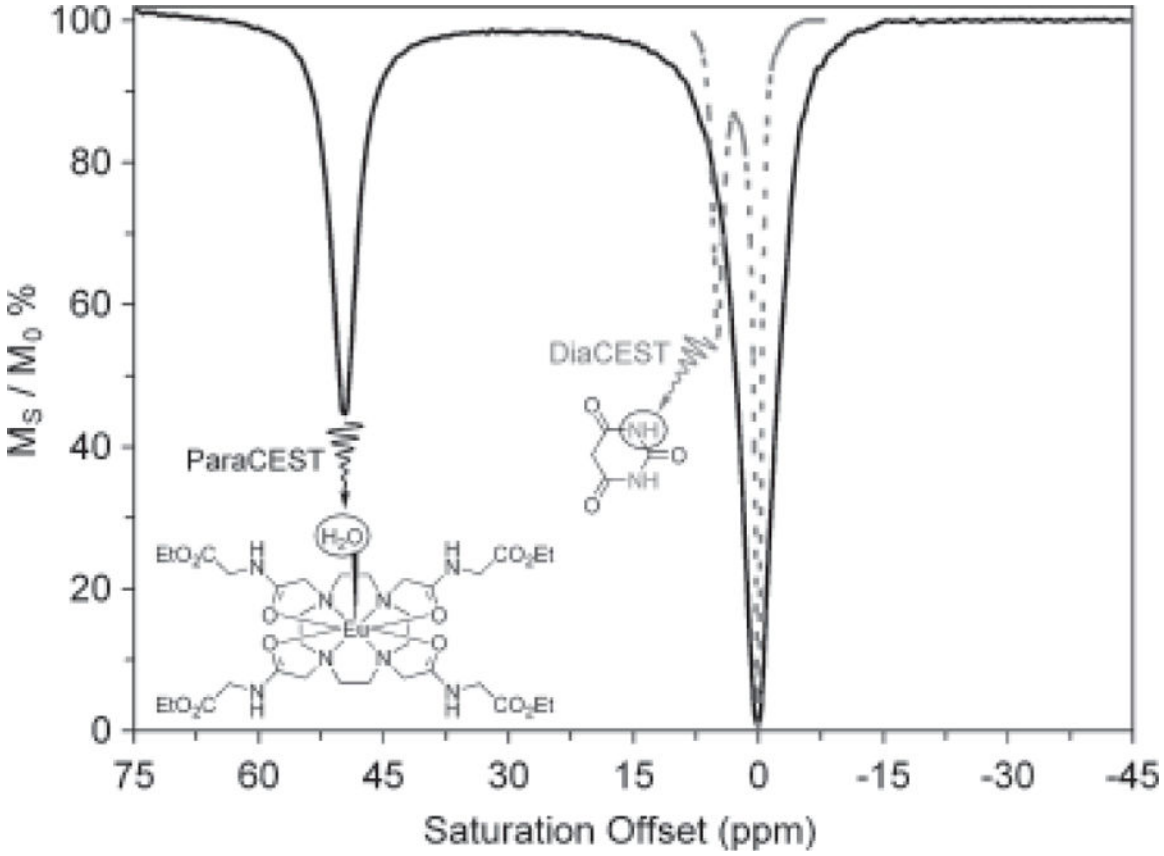

Fig. 2.

Comparison of CEST spectra for typical DIACEST and PARACEST agents. The dramatically larger Δω displayed by the PARACEST agent makes activation of the agent by an applied RF pulse less ambiguous.

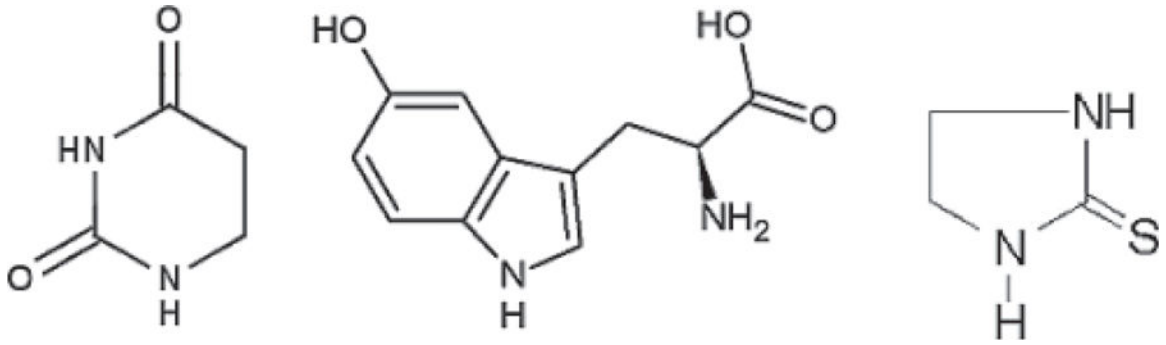

Fig. 3.

Chemical structures of small molecule DIACEST contrast agents, 5,6-dihydrouracil, 5-hydroxytryptophan, and 2-imidazolidinethione.

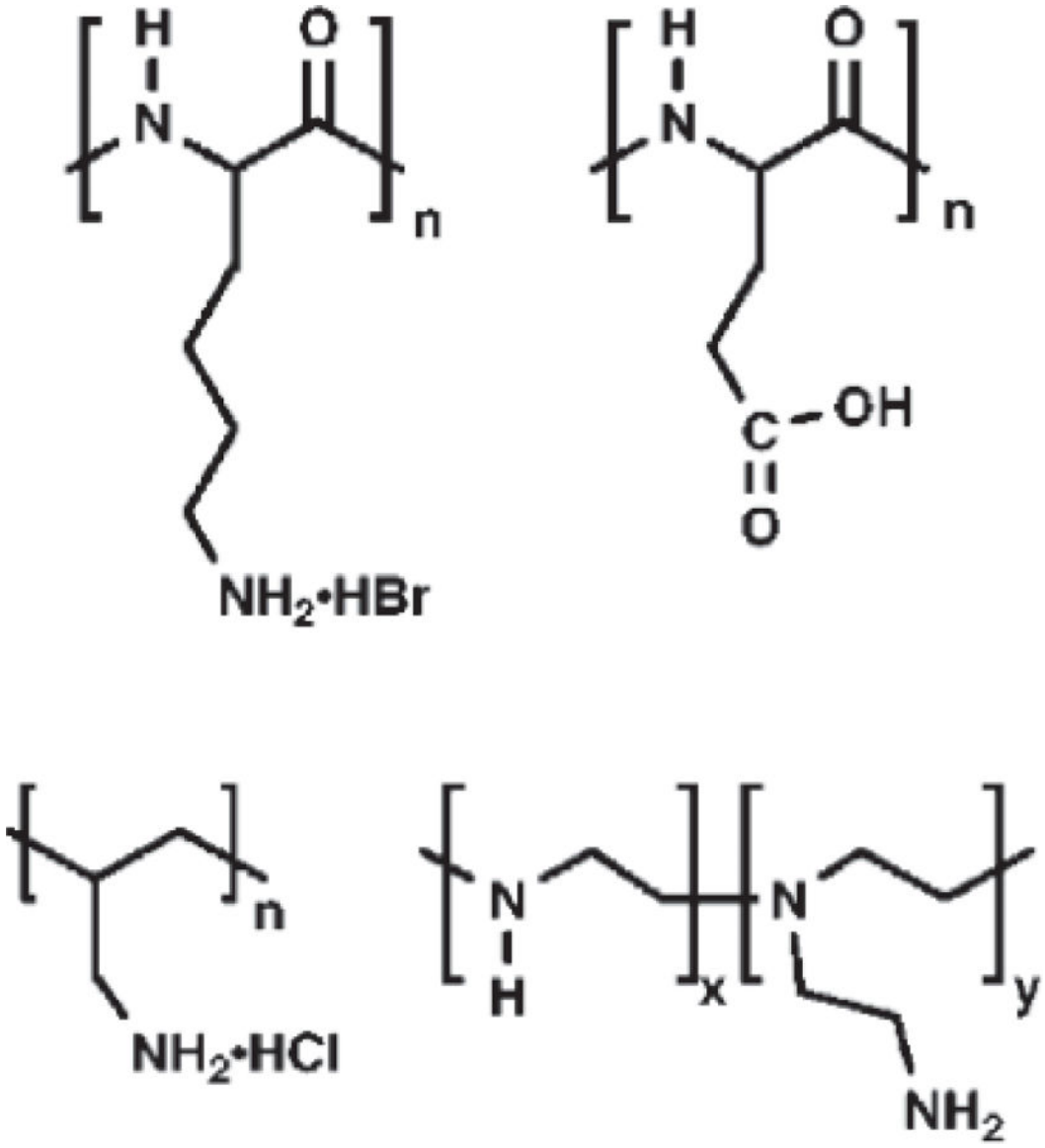

Fig. 4.

Chemical structures of macromolecular DIACEST contrast agents. From top left: poly-L-lysine (PLys), poly-L-glutamic acid (PGlu), polyallylamine, polyethylenimine (PEI).

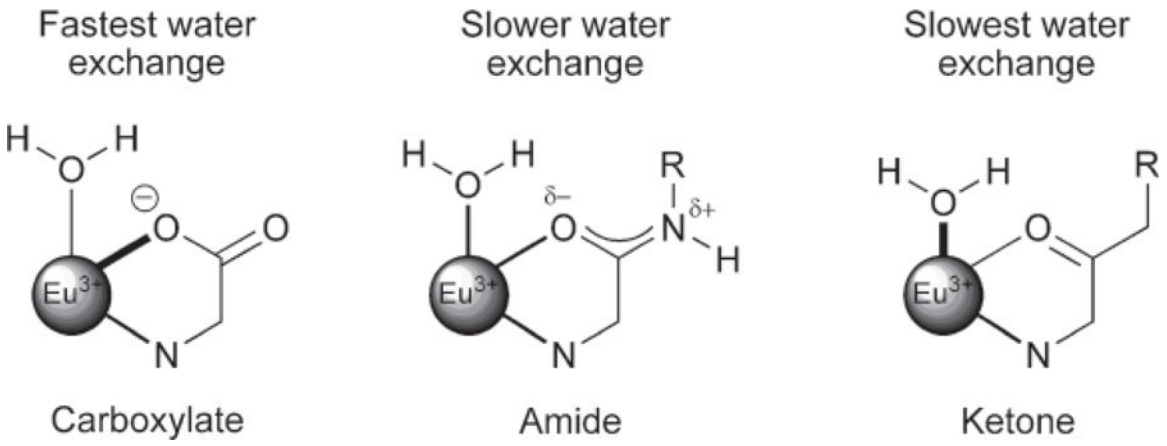

Fig. 5.

Electron delocalization from ligand oxygen donors to the lanthanide ion decreases in the donor series, carboxylates > amides > ketones. This results in the weakest Eu3+-water interaction in the carboxylate systems and faster water exchange. In the extreme, ketone-type ligands would contribute the least electron density, and thereby promote the strongest Eu3+-water interaction and slowest water exchange. Amide-containing systems fall between these extremes.

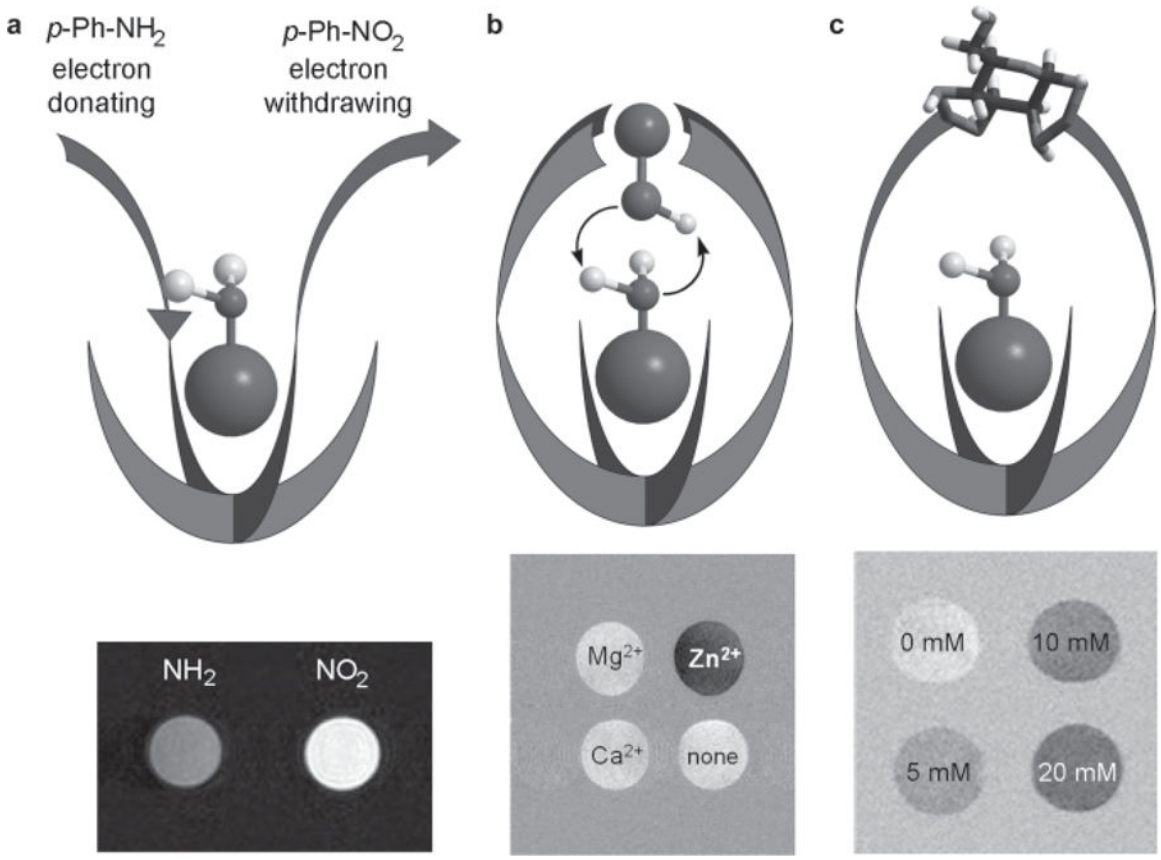

Fig. 6.

Illustrations of different ligand design concepts for “responsive” PARACEST agents. (a) Introduction of electron-withdrawing or electron-donating substituents into a single aromatic amide side-chain ligand alters water exchange and hence CEST. (b) At physiological pH the binding of Zn2+ to a site above the Eu3+-bound water molecule results in catalysis of proton exchange and “turns off “ CEST. (c) Binding of glucose over the Eu3+-bound water molecule slows water exchange and “turns on” CEST.

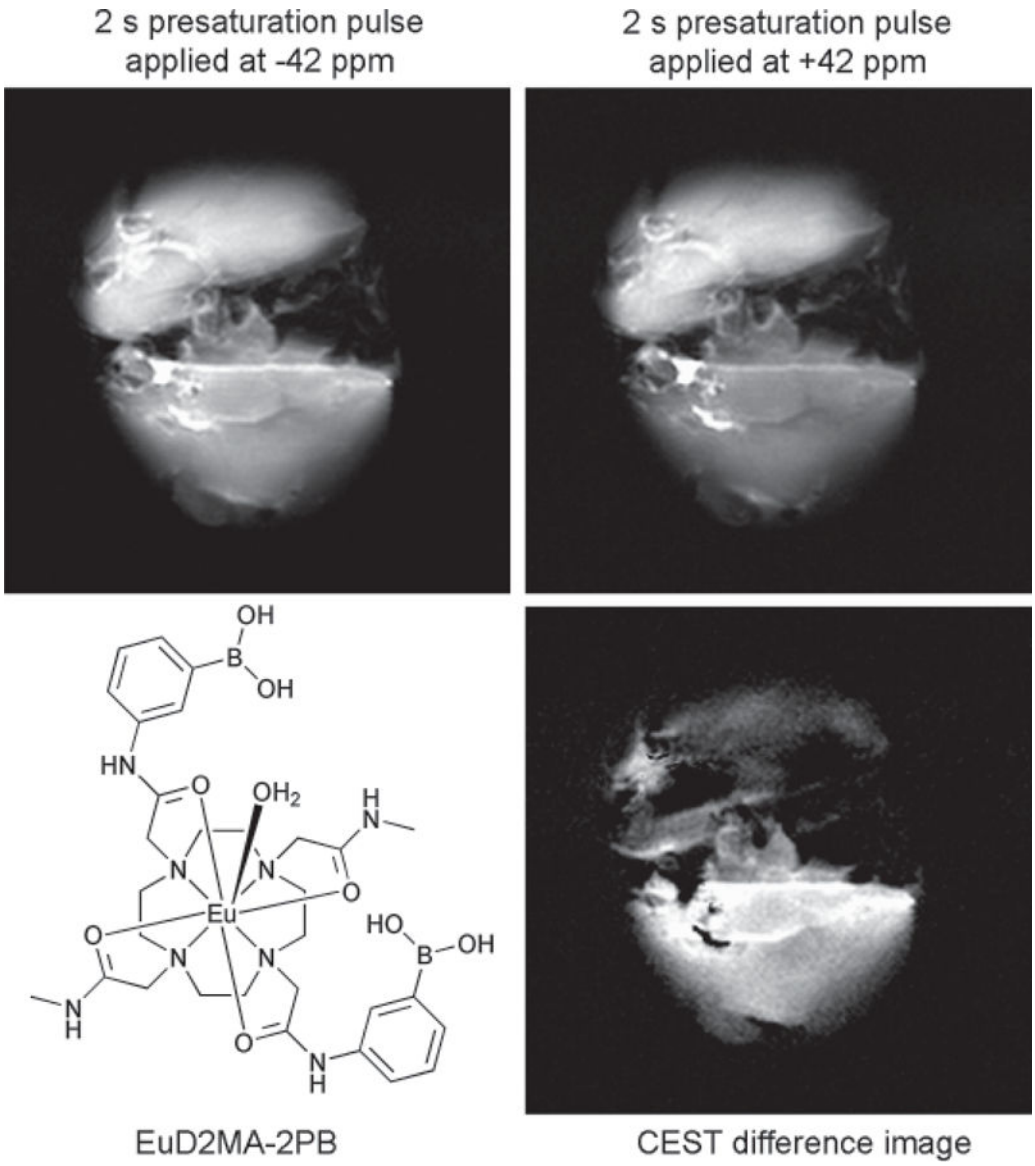

Fig. 7.

Ex vivo MR images of mouse livers (256 256 matrix, 40 40 mm field of view) after a bench perfusion with 10 mM EuX at 37C. The top liver in each panel was perfused without glucose, while the liver in the bottom of each panel was perfused with 10 mM glucose. The images were collected using a 4.7 T Varian Inova horizontal bore MR system with livers positioned over a 2.5 cm surface coil such that both livers could be imaged simultaneously. A spin-echo sequence with a Gaussian-shaped presaturation pulse (B1 peak power, 500 Hz; duration, 2 s) was used for imaging.

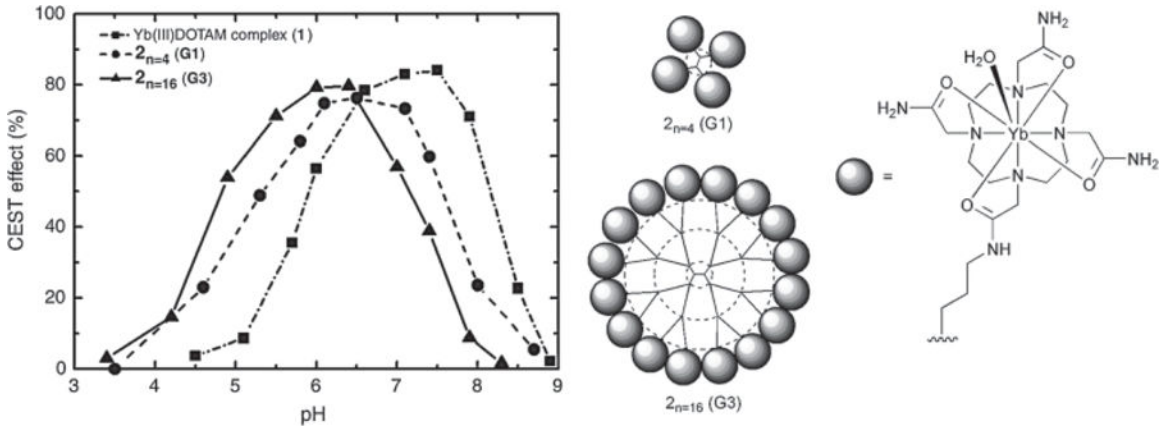

Fig. 8.

The amide protons of Yb-DOTAM complexes (structure on the right) exhibit a CEST effect that is highly pH dependent. By incorporating these PARACEST agents onto a dendrimer the pH range not only increases sensitivity but allows the pH range over which CEST changes to be tuned.

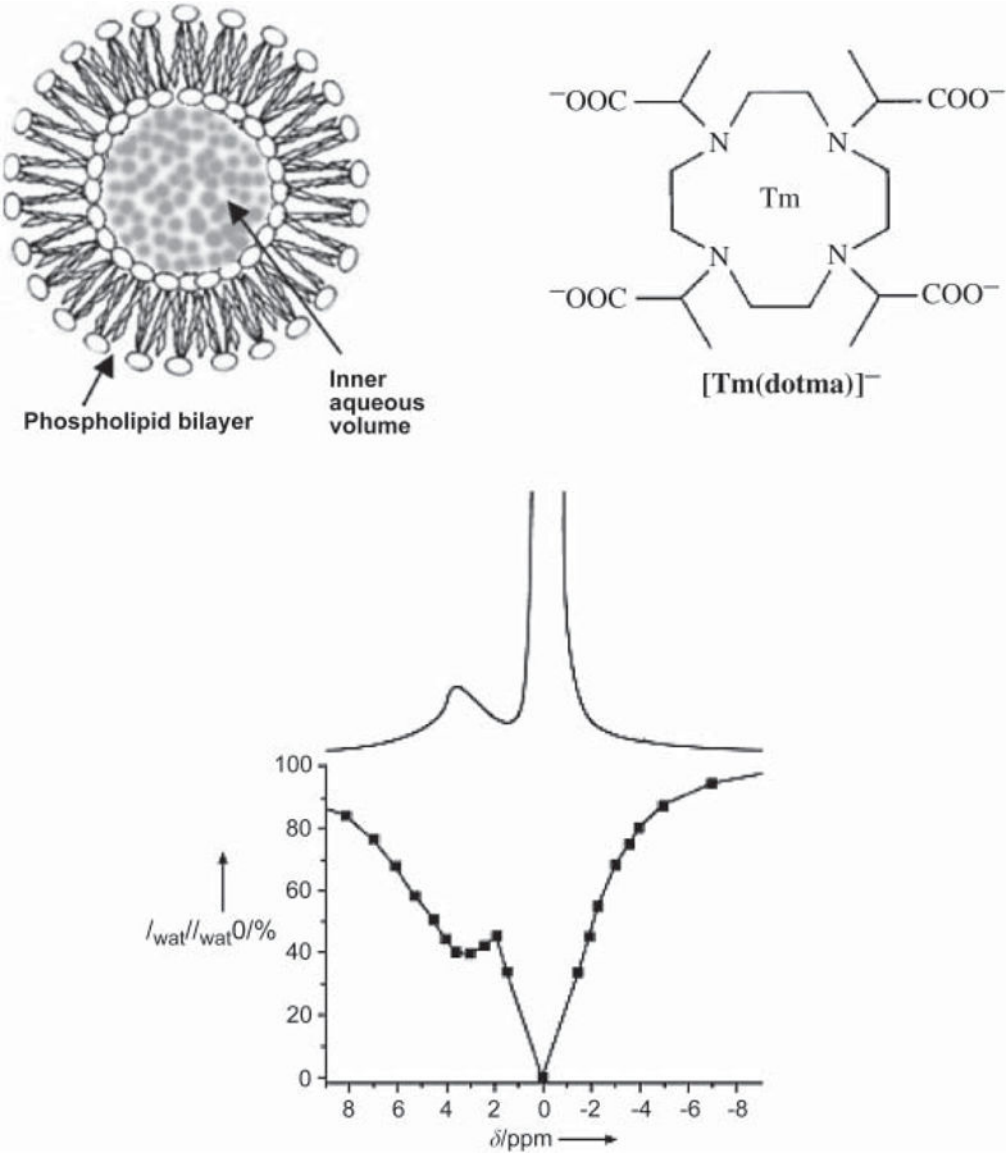

Fig. 9.

Schematic structure of large unilamellar phospholipid vesicles (liposomes, 100–300 nm), chemical structure of Tm-DOTMA, proton spectrum (upper curve), and Z spectrum (lower curve) of a suspension of vesicles; the vesicles contain 0.1 M of the agent, recorded at 600 MHz. Reproduced from TERRENO et al. (34).

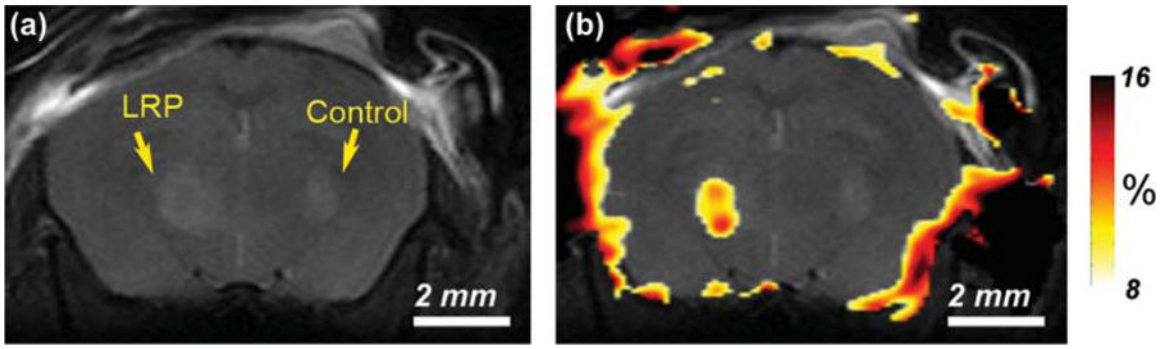

Fig. 10.

Images of mouse brain following inoculation with control and lysine-rich protein (LRP) expressing xenografts in opposite sides of the brain. (a) Anatomical image, (b) CEST signal intensity-difference map overlaid on the anatomical image. Reprinted with permission from Nat Biotechnol 2007.

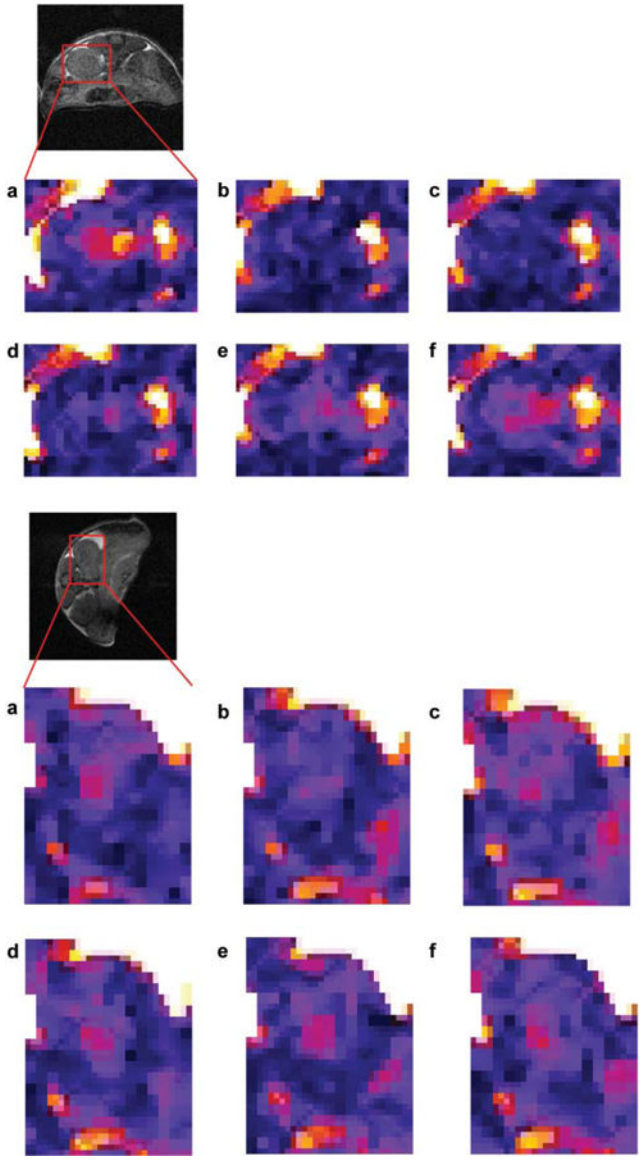

Fig. 11.

Typical WALTZ-SE images of the kidney zoomed in on the areas marked on the anatomical images. Images were taken just before or after 20 mM (top) or 2 mM (bottom) bolus injection of Tm-DOTAM-Gly (reproduced from Magn Reson Med 2007 with permission). (a) Before injection, and (b-f) after injection: (b) 2 min 40 s, (c) 5 min 20 s, (d) 10 min 40 s, (e) 16 min, (f) 18 min 40 s. All timings refer to the beginning of injection and beginning of image acquisition. It appears that maximum intensity is observed around 3 min (b). As the agent clears through the kidney, the intensity gradually returns to the preinjection level (d-f).

Table 1.

C_J values as reported by BLEANEY et al. (22, 23) are useful for predicting the relative magnitude of hyperfine shifts induced by the various lanthanide ions.

Ln^{3+}	Ce	Pr	Nd	Pm*	Sm	Eu	Gd	Tb	Dy	Ho	Er	Tm	Yb
Ionic Electronic configuration	$4f^1$	$4f^2$	$4f^3$	$4f^4$	$4f^5$	$4f^6$	$4f^7$	$4f^8$	$4f^9$	$4f^{10}$	$4f^{11}$	$4f^{12}$	$4f^{13}$
Unpaired electrons	1	2	3	4	5	6	7	6	5	4	3	2	1
C_J	− 6.3	− 11.0	− 4.2	2.0	− 0.7	4.0	0.0	− 86	− 100	− 39	33	53	22

*Unstable, radioactive.

Acta Radiol. Author manuscript; available in PMC 2019 June 26.